A DNA Oligonucleotide−Hemin Complex Cleaves *t*-Butyl Hydroperoxide through a Homolytic Mechanism

Paul K. Witting,[‡,†] Paula Travascio,[§] Dipankar Sen,*[,§] and A. Grant Mauk*[,‡]

Department of Biochemistry and Molecular Biology, University of British Columbia, Vancouver, British Columbia V6T 1Z3, Canada, and Institute of Molecular Biology and Biochemistry, Simon Fraser University, Burnaby, British Columbia V5A 1S6, Canada

Received January 8, 2001

Both electron paramagnetic resonance (EPR) and electronic absorption spectroscopy have been employed to investigate the reaction of a guanine-rich DNA nucleotide−hemin complex (PS2.M−hemin complex) and organic peroxide (*t*-Bu-OOH). Incubation of the PS2.M−hemin complex with *t*-Bu-OOH resulted in the time-dependent decrease in the heme Soret with concomitant changes to the visible bands of the electronic absorbance spectrum for the PS2.M−hemin complex. Parallel EPR studies using the spin trap 5,5-dimethyl-1-pyrroline *N*-oxide (DMPO) combined with spectral simulation demonstrated the presence of *tert*-butyloxyl, carbon-centered methyl, and methyl peroxyl radicals as well as a simple nitroxide (triplet) signal. Experiments, performed by maintaining a constant ratio of *t*-Bu-OOH/PS2.M−hemin complex (∼35 mol/mol) while varying DMPO concentration, indicated that the relative contributions of each radical adduct to the composite EPR spectrum were significantly influenced by the DMPO concentration. For example, at DMPO/PS2.M−hemin of 10−50 mol/mol, a complex mixture of radicals was consistently detected, whereas at high trapping efficiency (i.e., DMPO/PS2.M−hemin of ∼250 mol/mol) the *tert*-butyloxyl−DMPO adduct was predominant. In contrast, at relatively low DMPO/PS2.M−hemin complex ratios of ≤5 mol/mol, a simple nitroxide three-line EPR signal was detected largely in the absence of all other radicals. Together, these data indicate that *tert*-butyloxyl radical is the primary radical likely formed from the homolytic cleavage of the O−O peroxy bond of *t*-Bu-OOH, while methyl and methyl peroxyl radicals result from *β*-scission of the primary *tert*-butyloxyl radical product.

Introduction

Recent reports have provided a detailed kinetic analysis of the oligonucleotide−hemin complex-catalyzed (per)oxidation of 2,2′-azinobis(3-ethylbenzothiozoline)-6-sulfonic acid (ABTS)[1] in the presence of hydrogen peroxide (H_2O_2).[2,3] These studies on the reaction of hemin complexes of a specific guanine-rich DNA oligonucleotide (PS2.M) and corresponding RNA (rPS2.M) suggested that PS2.M and rPS2.M can act as ligands to bind and activate the heme iron for reaction with H_2O_2 (and ultimately catalyze the oxidation of substrates, e.g., ABTS) in the hemin-bound Michaelis complex.[4−6] The high percentage of guanine in PS2.M is necessary for the binding and activation of the heme prosthetic group.[2,3]

Low-temperature electron paramagnetic resonance spectroscopic (EPR)[7] investigations on the rest-state PS2.M−hemin complex indicated that the heme iron showed axial symmetry similar to myoglobin with a water molecule and guanine likely acting as the fifth and sixth axial ligands. Additionally, the pK_a (pK_a ≈ 8.7) determined for the acid−base transition of the complex was similar to that for horse heart myoglobin.[8] Also, treatment of the PS2.M−hemin complex with H_2O_2 yielded a radical exhibiting a singlet EPR signal. Parallel spin-trapping studies using 2-methyl-2-nitrosopropane (MNP) indicated that the free radical detected upon reactions of the PS2.M−hemin complex with H_2O_2 was either a tertiary or secondary carbon-centered radical, likely localized to the PS2.M oligonucleotide.[7]

Evidence for specific guanine base degradation on the PS2.M oligonucleotide after reaction with H_2O_2 further supported the idea that MNP trapped a carbon-centered radical potentially involved in the oxidative degradation of guanine bases.[7] Such oxidative damage to the matrix surrounding the heme prosthetic group is analogous to the translocation of oxidizing equivalents to the apoprotein of myoglobin[9−11] and hemoglobin[12,13] during

[‡] University of British Columbia.

[†] Current address: The Heart Research Institute, 145 Missenden Road, Camperdown, NSW 2050, Australia.

[§] Simon Fraser University.

(1) Abbreviations used are as follows: ABTS, 2,2′-azinobis(3-ethylbenzothiozoline)-6-sulfonic acid; RO•, alkoxyl radicals; DMPO, 5,5-dimethyl-1-pyrroline *N*-oxide; DTPA, diethylenetriamine pentaacetic acid; EPR, electron paramagnetic resonance spectroscopy; HRP, horseradish peroxidase; MES, 2-[*N*-morpholino]ethanesulfonic acid; CH_3•, methyl radical; CH_3OO•, methyl peroxyl radical; ROO•, alkyl peroxyl radical; PS2.M, guanine-rich oligonucleotide (5′-GTGGG-TAGGGCGGGTTGG-3′); PS2.M−hemin, DNA−hemin complex; *t*-Bu-OOH, *tert*-butyl hydroperoxide; *t*-Bu-O•, *tert*-butyloxyl radical; *t*-Bu-OO•, *tert*-butyl peroxyl radical; TEMPO, 2,2,6,6-tetramethyl-piperidine-*N*-oxyl; Tris, tris[hydroxymethyl]aminomethane.

(2) Travascio, P.; Bennet, A. J.; Wang, D. Y.; Sen, D. *Chem. Biol*. **1999**, *6*, 779−787.
(3) Travascio, P.; Li, Y.; Sen, D. *Chem. Biol*. **1998**, *5*, 505−517.
(4) Li, Y.; Sen, D. *Biochemistry* **1997**, *36*, 5589−5599.
(5) Sen, D.; Geyer, C. R. *Curr. Opin. Chem. Biol*. **1998**, *2*, 680−687.
(6) Li, Y.; Geyer, C. R.; Sen, D. *Biochemistry* **1996**, *35*, 6911−6922.
(7) Travascio, P.; Witting, P. K.; Mauk, A. G.; Sen, D. *J. Am. Chem. Soc*. **2001**, *123*, 1337−1348.
(8) Maurus, R.; Overall, C. M.; Bogumil, R.; Luo, Y.; Mauk, A. G.; Smith, M.; Brayer, G. D. *Biochim. Biophys. Acta* **1997**, *1341*, 1−13.
(9) Irwin, J. A.; Ostdal, H.; Davies, M. J. *Arch. Biochem. Biophys*. **1999**, *362*, 94−104.
(10) Gunther, M. R.; Tschirret-Guth, R. A.; Witkowska, H. E.; Fann, Y. C.; Barr, D. P.; Ortiz De Montellano, P. R.; Mason, R. P. *Biochem. J.* **1998**, *330*, 1293−1299.

10.1021/ic010025e CCC: $20.00
Published on Web 08/11/2001

protein-mediated H_2O_2 decomposition. Collectively, the evidence obtained from these previous studies supports the conclusion that the PS2.M−hemin complex acts as a peroxidase mimic. However, the precise mechanism for the reaction of the PS2.M−hemin complex with added peroxide was not demonstrated.

EPR has previously been employed to establish that heme proteins[14−18] and hemin alone[19] can react with organic peroxides to cleave the O−O bond and generate mixtures of organic free radicals. Although it is accepted that the oxidizing equivalents for the scission of the O−O bond generate a ferryl [Fe(IV)]-oxo species, there has been some controversy as to whether the O−O bond is cleaved by a process similar to the classical "peroxidase" mechanism (heterolysis), viz., yielding first an undetected porphyrin π-cation radical and an alcohol directly [reaction 1] and subsequently alkoxyl ($RO^\bullet$) and peroxyl ($ROO^\bullet$) radicals [reactions 2 and 3], by a homolytic process yielding $RO^\bullet$ as the primary product [reaction 4], or alternately by a hydrogen abstraction reaction yielding first peroxyl radicals ($ROO^\bullet$) and subsequently $RO^\bullet$ [reactions 5 and 6].

Heterolytic Mechanism

$$\text{protein}-\text{Fe(III)} + \text{ROOH} \rightarrow [\text{protein}-\text{Fe(IV)}{=}\text{O}]^{+\bullet} + \text{ROH} \quad (1)$$

$$[\text{protein}-\text{Fe(IV)}{=}\text{O}]^{+\bullet} + \text{ROOH} \rightarrow [\text{protein}-\text{Fe(IV)}{=}\text{O}] + \text{ROO}^\bullet + \text{H}^+ \quad (2)$$

$$\text{ROO}^\bullet + \text{ROO}^\bullet \rightarrow 2\text{RO}^\bullet + \text{O}_2 \quad (3)$$

Homolytic Mechanism

$$\text{protein}-\text{Fe(III)} + \text{ROOH} \rightarrow \text{protein}-\text{Fe(IV)}{=}\text{O} + \text{RO}^\bullet + \text{H}^+ \quad (4)$$

Metal-Mediated Hydrogen Abstraction Mechanism

$$\text{protein}-\text{Fe(III)} + \text{ROOH} \rightarrow \text{protein}-\text{Fe(II)} + \text{ROO}^\bullet + \text{H}^+ \quad (5)$$

$$\text{protein}-\text{Fe(II)} + \text{ROOH} \rightarrow \text{protein}-\text{Fe(III)} + \text{RO}^\bullet + \text{OH}^- \quad (6)$$

In this study, we have employed EPR to investigate the mechanism of organic peroxide decomposition by the hemin complex of PS2.M oligonucleotide and now show that a mixture of free radicals is produced from reaction of *t*-Bu-OOH with PS2.M−hemin complex.

Experimental Section

Materials. 5,5-Dimethyl-1-pyrroline *N*-oxide (DMPO), *tert*-butyl hydroperoxide (*t*-Bu-OOH), 2,2,6,6-tetramethylpiperidine-*N*-oxyl (TEMPO), EDTA, Triton-100, diethylenetriaminepentaacetic acid (DTPA), tris[hydroxymethyl]aminomethane (Tris), and 2-[*N*-morpholino]ethanesulfonic acid (MES) were obtained from Sigma (St. Louis, MO). DMPO (1 M in phosphate buffer, 50 mM, pH 7.4) was purified before use by stirring with activated charcoal (100 mg/mL) in the dark.[20] H_2O_2 (30% w/v) was from BioRad (Richmond, CA). Hemin was from Porphyrin products (Logan, Utah) and was used without purification. Solutions of hemin (≤2 mM) were prepared by dissolving the porphyrin in 0.01 M NaOH. Solutions of PS2.M−hemin complex were freshly prepared for each study by diluting the hemin stock solution into the appropriate buffers containing the PS2.M oligonucleotide (see below). Buffers were prepared from either glass-distilled water or glass-distilled water purified further by passage through a Barnstead Nanopure system. All buffers were stored over Chelex-100 (BioRad) at 4 °C for at least 24 h to remove contaminating transition metals as verified by the ascorbate autoxidation analysis.[21] All chemicals and solvents employed were of the highest quality available.

Preparation of DNA−Hemin Complexes. The guanine-rich PS2.M oligonucleotide (5′-GTGGGTAGGGCGGGTTGG-3′) was synthesized at the University Core DNA Service at the University of Calgary. Crude preparations of the oligonucleotide were size-purified in preparative polyacrylamide and repurified on Spice C18 columns as described.[1,2] After lyophilization, purified PS2.M was dissolved in TE buffer (10 mM Tris, pH 7.5 with 0.1 mM EDTA) and stored at −80 °C until required. Solutions of PS2.M oligonucleotide were standardized from absorbance at A_{260nm} (with 1 OD taken to be 35−40 μg/mL of DNA oligonucleotide). When required, aliquots of PS2.M were first thawed at 20 °C and then heated at 95 °C for 5 min. Next, the oligonucleotide was diluted using 100 mM MES buffer (pH 6.3 containing 50 mM Tris, 40 mM KCl, 1% DMSO v/v, and 0.05% Triton-100 v/v) and allowed to stand for 30 min at room temperature. Finally, hemin (25 mM in 0.01 M NaOH) was added to the oligonucleotide (at PS2.M/hemin ratio of 2:1 mol/mol), and the mixture was gently mixed for 20 min at 20 °C to yield the PS2.M−hemin complex. Thus, the DNA oligonucleotide was present in 2-fold excess of added hemin. Peroxidation assays were carried out with ratios of PS2.M−hemin complex/*t*-Bu-OOH as indicated in the legends to the figures.

EPR Spectroscopy. X-band EPR spectra (293 K) were obtained with a Bruker ESP 300e spectrometer equipped with a Hewlett-Packard frequency counter. Where required, solutions of the PS2.M−hemin complex (~1 mM in MES buffer, 100 mM, pH 6.3 containing 50 mM Tris, 40 mM KCl, 1% DMSO v/v, and 0.05% w/v Triton-100) were treated with *t*-Bu-OOH at ratios of PS2.M−hemin/*t*-Bu-OOH = 1:35 mol/mol in both the presence and absence of DMPO (PS2.M−hemin complex/DMPO ratio indicated in the legend to the figures). Analyses of DMPO adducts were performed on aliquots (50 μL) of the reaction mixture transferred into capillary tubes with a glass pipet. The capillary was then placed into a quartz EPR tube and transferred to the cavity for analyses at 293 K. The limit of detection of a stable nitroxide (TEMPO) was determined to be ~50 nM under identical conditions. Unless indicated otherwise, the time between removal of the sample, transfer to the appropriate cell, and tuning the spectrometer was consistently less than 30 s. Spectra were obtained as an average of five scans with a modulation frequency of 100 kHz and a sweep time of 84 s. Microwave power, modulation amplitude, and scan range used for each analysis varied appropriately as indicated in the figure legends. Peak area was estimated by double integration using standard WINEPR software. DTPA (100 μM) was included in all solutions prior to the addition of *t*-Bu-OOH to minimize the possibility of transition-metal-mediated decomposition of peroxide by Fenton chemistry. Anaerobic analyses were performed by degassing solutions with purified nitrogen gas that had previously passed through a vanadium(II)/mercury−zinc-amalgam bubbler as described.[22] Transfer of degassed reactants and reaction mixtures was carried out using gastight syringes and rubber septa to avoid oxygen contamination.

Computer Simulation of EPR Spectra. Hyperfine couplings were obtained by spectral simulation using the simplex algorithm[23] provided

(11) Tschirret-Guth, R. A.; Ortiz de Montellano, P. R. *Arch. Biochem. Biophys*. **1996**, *335*, 93−101.
(12) Svistunenko, D. A.; Patel, R. P.; Voloshchenko, S. V.; Wilson, M. T. *J. Biol. Chem*. **1997**, *272*, 7114−7121.
(13) McArthur, K. M.; Davies, M. J. *Biochim. Biophys. Acta* **1993**, *1202*, 173−181.
(14) Rota, C.; Barr, D. P.; Martin, M. V.; Guengerich, F. P.; Tomasi, A.; Mason, R. P. *Biochem. J*. **1995**, *328*, 565−571.
(15) Barr, D. P.; Martin, M. V.; Guengerich, F. P.; Mason, R. P. *Chem. Res. Toxicol.* **1996**, *9*, 318−325.
(16) Greenley, T. L.; Davies, M. J. *Biochim. Biophys. Acta* **1992**, *1116*, 192−203.
(17) Davies, M. J. *Biochim. Biophys. Acta* **1988**, *964*, 28−35.
(18) Timmins, G. S.; Davies, M. J.; Song, D. X.; Muller-Eberhard, U. *Free Radical Res*. **1995**, *23*, 559−569.
(19) Van der Zee, J.; Barr, D. P.; Mason, R. P. *Free Radical Biol. Med.* **1996**, *20*, 199−206.
(20) Kotake, Y.; Reineke, L. A.; Tanigawa, T.; Koshida, H. *Free Radical Biol. Med*. **1994**, *17*, 215−223.
(21) Buettner, G. R. *Methods Enzymol*. **1990**, *186*, 125−127.
(22) Meites, L.; Meites, T. *Anal. Chem*. **1948**, *20*, 984−985.

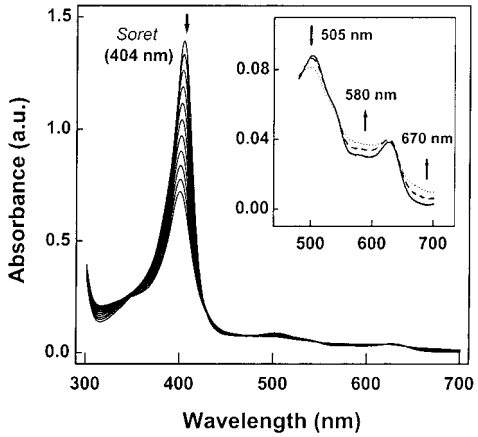

Figure 1. Time-dependent decay of the Soret and visible maxima for reaction of PS2.M−hemin complex (2 μM) with *t*-Bu-OOH (ratio of *t*-Bu-OOH/PS2.M−hemin of ∼5 mol/mol). Reaction mixtures were incubated at 20 °C, and spectra were obtained at 1 min intervals. Where shown, arrows indicate the direction of the change in absorbance. Inset shows spectra measured over the visible region after 1 min (filled line), 4 min (dashed line), and 8 min (dotted line). Data represent three or more experiments with different PS2.M−hemin complex preparations.

in "WINSIM" software that is available for use at the NIEHS/NIH website (URL, http://epr.niehs.nih.gov/). Hyperfine couplings are expressed in units of millitesla. Simulations were considered acceptable at correlation factors of $R > 0.85$. Computer simulations of the experimental data obtained at various ratios of DMPO/PS2.M−hemin complex were also used to determine the relative concentration of each radical adduct for each composite EPR spectrum. Relative concentrations of individual components were determined by first identifying the clearly resolved low-field absorption of each species in the various spectra by using spectral simulation. Next, the low-field EPR signals of individual components were double integrated to give a relative mole fraction of the particular DMPO adduct in the composite mixture at a given ratio of DMPO/PS2.M−hemin complex.

Electronic Absorption Spectra. The spectral changes of PS2.M−hemin (or hemin alone) were recorded using a Cary 300 Bio UV−visible spectrophotometer. The reactions were initiated by the addition of *t*-Bu-OOH at 20 °C. Further details are provided in the legend to the figure.

Results

Electronic Absorption Spectroscopy. The time-dependent changes to the Soret and visible absorption bands of the ferric form of the PS2.M−hemin complex upon *t*-Bu-OOH addition are shown in Figure 1. The rest-state complex showed a Soret band at 404 nm and weaker maxima over the visible range of 480−700 nm characteristic of a high-spin ferric state.[3] Addition of *t*-Bu-OOH (*t*-Bu-OOH/PS2.M−hemin complex ≈ 200 mol/mol) resulted in a time-dependent bleaching of the Soret with isosbestic points at A_{348nm} and A_{428nm}. Significant changes to the visible bands were also detected over the period monitored. Overall, the Soret intensity was decreased (by a factor of ∼2) while changes to the visible region included a decrease at A_{505nm} and increases at A_{580nm} and A_{670nm} (see Figure 1, inset). Collectively, these results are consistent with corresponding reactions of the horseradish peroxidase (HRP)[24,25] and prostaglandin H synthase[26] with H_2O_2, in which the formation of compound I is reportedly characterized by similar changes to Soret and visible bands upon reaction with peroxide. The spectrum derived from the reaction of the PS2.M−hemin complex with *t*-Bu-OOH was also significantly different from that of an Fe(IV)-ferryl species (i.e., compound II) of both HRP and prostaglandin H synthase that exhibits a Soret band with peak intensity slightly greater than that of the native protein and is red-shifted relative to Soret maxima of the rest state.[26] Moreover, the low molar absorbitivities in the Soret region of the H_2O_2 derivatives of HRP and some other hemoproteins (i.e., catalase and chloroperoxidase) are considered as indicative of the formation of a porphyrin π-radical cation.[27] The lack of a shift in the Soret maxima of PS2.M−hemin complex upon treatment with *t*-Bu-OOH would suggest that a compound II-like intermediate is not detected under these conditions. The latter observation is not necessarily uncommon as similar behavior has been reported for cytochrome C[28−30] for which a compound I intermediate is thought by some[17,25] though not all[15,28] to result in the catalytic decomposition of peroxide. Importantly, no free hemin (maximum at A_{398nm}) was detected in mixtures of the PS2.M oligonucleotide and hemin either before or after addition of peroxide, indicating that all of the added heme remained bound to the oligonucleotide.

Spin-Trapping Investigations on the Reaction of PS2.M−Hemin Complex and *t*-Bu-OOH. The reaction of the PS2.M−hemin complex with *t*-Bu-OOH was also studied by EPR spectroscopy in combination with spin trapping. Aerobic addition of DMPO to the reaction at ratios of PS2.M−hemin complex/*t*-Bu-OOH/DMPO of ∼1:35:10−50 mol/mol/mol, consistently gave a complex mixture of radical adducts (e.g., see Figure 2). This mixture of radicals contained components similar to those observed previously for reactions of heme proteins and organic hydroperoxides.[15−18,28,31] In contrast, no EPR signals were detected in the absence of DMPO, *t*-Bu-OOH, or the PS2.M−hemin complex indicating that either no radical adducts were produced under these conditions or that when formed, the DMPO adducts were below the limit (i.e., yields of radical adduct of less than 50 nM) of detection (Figure 2B−D).

Addition of DMPO to mixtures of hemin and *t*-Bu-OOH in the absence of PS2.M oligonucleotide also resulted in the detection of radical adducts under identical reaction conditions (Figure 2E). Simulations of the EPR signals obtained in the absence of the oligonucleotide indicated the presence of a mixture of radical adducts (not shown). The major component of the mixture showed coupling to single nitrogen (a^N) and hydrogen atoms (a^H_β) with hyperfine coupling constants of $a^N = 0.70$ and $a^H_\beta = 0.38$ mT. These hyperfine couplings are similar to that previously reported for 5,5-dimethyl-2-pyrrolidone-*N*-oxyl (DMPOX),[10,31] an oxidation product of DMPO, and so this radical was assigned as DMPOX. A second weaker DMPO adduct (see arrows in Figure 2E) showed couplings of $a^N = 1.51$ and $a^H_\beta = 1.45$ mT, consistent with the assignment of a hydroxyl radical adduct of DMPO (DMPO−OH).[32] No other radical adducts were detected under these conditions. Residual DMSO (present in the final buffer mixture) can be an effective trap for hydroxyl radicals yielding methyl radicals or formaldehyde or both.[33] Importantly, the detection of DMPO−

(23) Duling, D. R. *J. Magn. Reson*. **1994**, *104B*, 105−110.
(24) Chance, B. *Arch. Biochem. Biophys*. **1949**, *21*, 416−430.
(25) Dunford, H. B. *Coord. Chem. Rev*. **1976**, *19*, 187−251.
(26) Dunford, H. B. *Heme Peroxidases*; Wiley & Sons Inc: New York, 1999; p 389.
(27) Ortiz de Montellano, P. R. *Cytochrome P450*; Wiley: New York, 1986.
(28) Barr, D. P.; Mason, R. P. *J. Biol. Chem*. **1995**, *270*, 12709−12716.
(29) Harel, S.; Salan, M. A.; Kanner, J. *Free Radical Res. Commun*. **1988**, *5*, 11−19.
(30) Harel, S.; Kanner, J. *Free Radical Res. Commun*. **1988**, *5*, 21−33.
(31) Thornalley, P. J.; Trotta, R. J.; Stern, A. *Biochim. Biophys. Acta* **1983**, *759*, 16−22.
(32) Sargent, F. P.; Gardy, E. M. *Can. J. Chem*. **1976**, *54*, 275−279.
(33) Rosen, G. M.; Britigan, B. E.; Halpern, H. J.; Sovitj, P. *Free Radicals: Biology and Detection by Spin Trapping*; Oxford University Press: New York and Oxford, 1999; p 148.

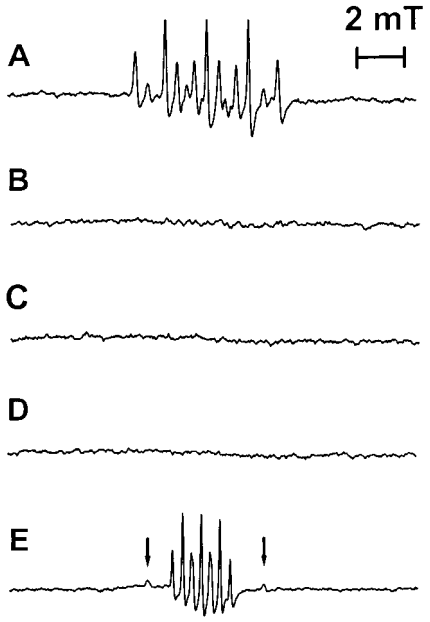

Figure 2. Panel A shows the EPR spectrum obtained from a mixture of PS2.M−hemin complex, *t*-Bu-OOH, and the spin trap DMPO at a ratio of 1:35:10 mol/mol/mol after 2 min reaction at 20 °C. No EPR signal was detected in the absence of (B) DMPO, (C) PS2.M−hemin, or (D) *t*-Bu-OOH. In contrast, *t*-Bu-OOH added to hemin and DMPO in the absence of PS2.M (E) yields a mixture of radicals. Arrows in panel E indicate outlying EPR lines for DMPO−OH. Spectra represent an average of five scans and were obtained with microwave power of 100 mW, modulation amplitude of 0.1 mT, modulation frequency of 100 kHz, sweep width of 16 mT, sweep time of 84 s, and time constant of 1.3 s. Solutions of PS2.M−hemin complex contained 100 μM DTPA. Data represent three or more experiments with different preparations of the PS2.M−hemin complex.

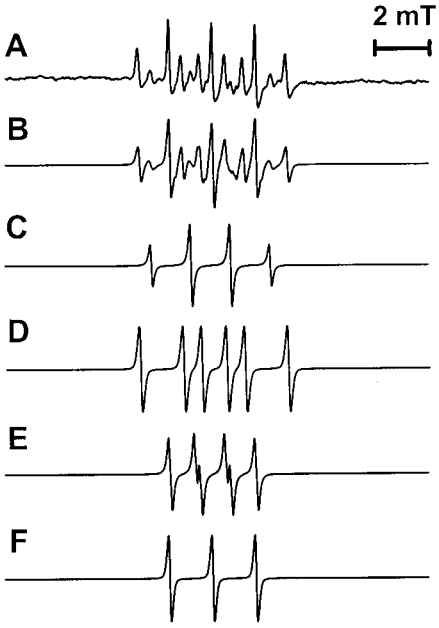

Figure 3. Composite EPR spectra from reaction mixtures of PS2.M−hemin complex, *t*-Bu-OOH, and the spin trap DMPO at a ratio of 1:35:10 mol/mol/mol (A), readily simulated to good fit (B) with a correlation factor $R > 0.85$. Individual components of the composite spectra are assigned as DMPO radical adducts of (C) *tert*-butyloxyl, (D) methyl, (E) methyl peroxyl, and (F) a simple nitroxide species. Simulations were performed with "WINSIM" software[23] (see Experimental Section). EPR parameters were as for Figure 2. All solutions of the PS2.M−hemin complex contained 100 μM DTPA. Data represent three or more experiments.

OH indicates that residual DMSO (<1% v/v) present in the buffer does not compete with DMPO for the trapping of hydroxyl radical and is therefore unlikely to contribute to the composite EPR spectra obtained from reaction mixtures of PS2.M−hemin and *t*-Bu-OOH.

EPR Spectral Simulations of Composite Spectra. To assign identity to the radicals comprising the complicated composite EPR spectra from the reaction mixtures of PS2.M−hemin/*t*-Bu-OOH/DMPO in ratios of ~1:35:10−50 mol/mol/mol, the spectra were first separated into individual components by spectral simulation (Figure 3). Overall, the composite mixture of DMPO adducts obtained from a reaction of PS2.M−hemin complex, *t*-Bu-OOH, and DMPO (e.g., Figure 3A) was readily simulated with good fits to the experimental data (e.g., Figure 3B). Table 1 reports the hyperfine couplings from individual EPR simulations (e.g., Figure 3 C−E) of the various DMPO adducts used to generate the final simulation of the composites spectra together with coupling values from known DMPO adducts.

A comparison of hyperfine values from the data obtained in this study with literature values (Table 1) suggests the following assignment of identity to the DMPO adducts detected: *tert*-butyloxyl- (Figure 3C), peroxyl- (Figure 3D), and carbon-centered radicals (Figure 3E). In addition to these radicals, a triplet signal was also required to adequately simulate the composite spectra (Figure 3F). Interestingly, the sharp three-line spectrum exhibited a line width of less than 0.01 mT indicating that if the triplet were to arise from a radical adduct of DMPO then hyperfine coupling to the β-hydrogen of DMPO must either be less than or equal to 0.01 mT or not present at all. Such a radical adduct has not been previously described for DMPO indicating that this radical is likely a simple free nitroxide radical.

Oxygen-Dependence on DMPO Radical Adduct Formation. Peroxyl radicals derived from *t*-Bu-OOH may arise from one or all of the processes described by reactions 7−9 where β-scission of the *tert*-butyloxyl radical (*t*-BuO$^\bullet$) gives rise to the carbon-centered methyl radical ($CH_3^\bullet$).

$$CH_3^\bullet + O_2 \rightarrow CH_3OO^\bullet \quad (7)$$

$$CH_3^\bullet + t\text{-Bu-OOH} \rightarrow CH_4 + t\text{-BuOO}^\bullet \quad (8)$$

$$t\text{-BuO}^\bullet + t\text{-Bu-OOH} \rightarrow t\text{-BuOH} + t\text{-BuOO}^\bullet \quad (9)$$

EPR analyses of DMPO−peroxyl radical adducts cannot discriminate between adducts derived from methyl ($CH_3OO^\bullet$) or *tert*-butyl peroxyl (*t*-BuOO$^\bullet$) radicals. Thus, the precise identity of the peroxyl radical adduct detected in reaction mixtures of PS2.M−hemin and *t*-Bu-OOH cannot be immediately assigned from the available data. Therefore, to assign identity to these radical adducts, we investigated spin-trapping experiments in both the presence and absence of oxygen (Figure 4). In the absence of dioxygen, and with a relatively low dose of DMPO employed to optimize detection of peroxyl radicals, the formation of the radical adduct assigned as a DMPO−peroxyl radical (▼ in Figure 4) was decreased relative to the *tert*-butyloxyl radical adduct (● in Figure 4) (cf. parts A and B of Figure 4). In addition, the intensity of the DMPO adduct assigned as derived from a carbon-centered radical (▲ in Figure 4) and the nitroxide radical (■ in Figure 4) increased marginally in the absence of dioxygen (cf. parts A and B of Figure 4). Together, these data support the argument that the formation of the peroxyl radical is dependent on the presence of dioxygen.

Table 1. Hyperfine Coupling Constants for Various DMPO Adducts Obtained from the Reactions of Heme Proteins or Heme Complexes and *t*-Bu-OOH[a]

adduct	a^N	a^H_β	a^H_γ	reference
tert-butyloxyl	1.49 ± 0.01	1.63 ± 0.01		16, 17, 27, 30, 38
cumyloxyl	1.48 ± 0.01	1.54 ± 0.04		14, 27, 39
cumenyl peroxyl	1.45	1.08	0.18	40
methyl peroxyl	1.44 ± 0.01	1.07 ± 0.01	0.14 ± 0.01	16, 17, 27, 30, 38
ethyl peroxyl	1.46	1.10	0.13	41
methyl	1.65 ± 0.01	2.35 ± 0.01		16, 17, 27, 30, 38
alkoxyl	1.49 ± 0.01	1.58 ± 0.03		this work
peroxyl	1.43 ± 0.03	1.11 ± 0.01	0.09 ± 0.03	this work
alkyl	1.62 ± 0.05	2.25 ± 0.05		this work
triplet	1.62 ± 0.02			this work

[a] Hyperfine coupling constants are given as data from a single literature source or as mean ± SD of literature values or where indicated are obtained from the current study. Hyperfine coupling values determined in this study were optimized by simulation using WINSIM software,[23] accepting correlation coefficients of $R > 0.85$. Data shown represent mean ± SD of at least three independent studies using different preparations of PS2.M−hemin complex. All values are given in units of millitesla. Where data are not shown, the coupling constant is not applicable.

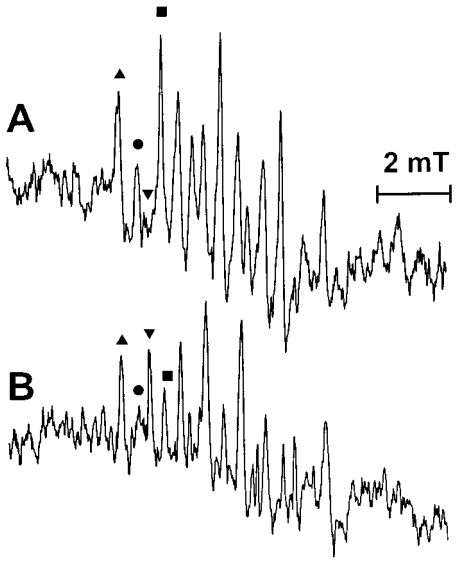

Figure 4. The PS2.M−hemin complex was treated with *t*-Bu-OOH in the presence of DMPO (ratio of PS2.M−hemin complex/*t*-Bu-OOH/DMPO 1:35:20 mol/mol/mol) in either (A) the absence or (B) the presence of dioxygen. DMPO radical adducts are marked with the following symbols at well-resolved low-field absorptions: (▲) methyl, (●) butyloxyl, (▼) methyl peroxyl, and (■) nitroxide radicals. EPR parameters were as for Figure 2. Each plot is presented with an identical vertical intensity scale for direct comparison of changes in peak intensity. All solutions of the PS2.M−hemin complex contained 100 μM DTPA.

Thus, the peroxyl radical detected here is likely generated by reaction of the carbon-centered radical and oxygen [reaction 7] and not by simple hydrogen abstraction from *t*-Bu-OOH [reactions 8 and 9], as the latter process does not involve a dependence on dioxygen. The observed increase in the DMPO adduct of carbon-centered radicals under anaerobic conditions that inhibit its conversion to a peroxyl radical also supports this conclusion. On the basis of these oxygen-dependent studies, we assigned the peroxyl and the carbon-centered radicals as methyl and methyl peroxyl radicals, respectively.

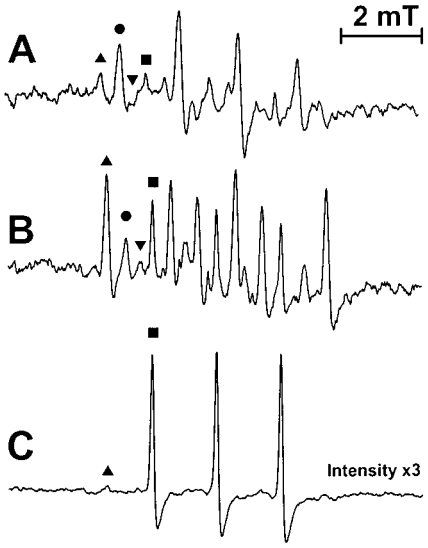

Figure 5. Composite EPR spectra obtained from the reaction of the PS2.M−hemin complex and *t*-Bu-OOH in the presence of (A) 250, (B) 50, and (C) 5 mM DMPO. EPR parameters were as for Figure 2. Plots A and B are presented with an identical vertical intensity scale for direct comparison of changes in peak intensity, while spectrum C is plotted with a 3-fold larger scale. Symbols indicating the well-resolved low-field lines of the various DMPO adducts are as for Figure 4. All solutions of the PS2.M−hemin complex contained 100 μM DTPA.

Effect of Increasing Spin-Trapping Efficiency on the Yield of DMPO Adducts. As indicated in the Introduction, there are several mechanisms that may give rise to a mixture of free radicals from the decomposition of *t*-Bu-OOH. To obtain further information on which of the possible mechanisms yields the DMPO adducts detected here, we next investigated the effect of increasing DMPO trapping efficiency (i.e., increasing the DMPO/PS2.M−hemin complex ratio) while maintaining the ratio of *t*-Bu-OOH/PS2.M−hemin at ∼35 mol/mol on the formation of the various radical adducts (Figure 5). Secondary reactions that lead to the formation of radicals after the generation of an initial primary radical can be suppressed by simply increasing the spin-trap concentration. Thus, under conditions of high trapping efficiency, the primary radical species produced in the reaction can be identified. Figure 5 shows that increasing the dose of DMPO (from 5 to 250 mM) results in a marked decrease and increase for the relative intensities of methyl peroxyl (▼ in Figure 5) and *tert*-butyloxyl (● in Figure 5) adducts, respectively (cf. parts A and B of Figure 5). At the lowest concentration of spin trap investigated (5 mM) a sharp triplet (■ in Figure 5) EPR signal ($a^N = 1.62$ mT) was detected (Figure 5C). Under these conditions, the only other radical detected was the DMPO−methyl adduct (▲ in Figure 5) in low yield (Figure 5C). The triplet signal detected under these conditions was identical to that required for the accurate simulation of the composite spectra (vide infra). The intensity of the triplet signal also decreased with increasing dose of DMPO (cf. Figure 5A−C). Changes to the DMPO−methyl radical adduct were less marked, and this species was detected at all concentrations (albeit in decreasing relative concentration) of DMPO tested. Double integration of the clearly resolved EPR absorptions of each individual component of the composite spectrum afforded estimates of the relative fraction of each radical adduct at each of the DMPO concentrations investigated (Figure 6). Clearly, the relative mole fraction of DMPO−methyl and DMPO−methyl peroxyl radicals and the nitroxide reached maximal concentrations at [DMPO] ≤ 20 mM. Subsequently,

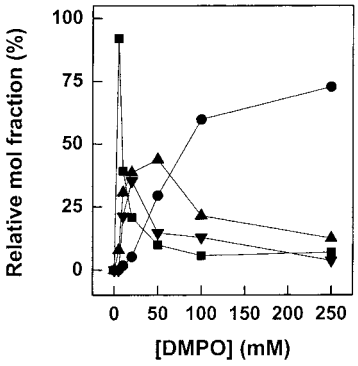

Figure 6. Changes to each component from the composite EPR spectra with increasing spin trap determined by double integration and plotted as the relative mole fraction as a function of DMPO concentration (mM). The concentration of *t*-Bu-OOH was maintained at *t*-Bu-OOH/PS2.M−hemin complex ratio of ∼35 mol/mol for all concentrations of DMPO investigated. DMPO radical adducts are marked as follows: (▲) methyl, (●) butyloxyl, (▼) methyl peroxyl, and (■) nitroxide. EPR parameters were as for Figure 2. All solutions of the PS2.M−hemin complex contained 100 μM DTPA.

the relative mole fraction of these radical adducts decreased in the range of 20 mM < [DMPO] ≤ 250 mM. In contrast, the relative mole fraction of the radical adduct derived from trapping *tert*-butyloxyl radicals increased significantly over all DMPO concentrations tested.

Discussion

Recently, we showed that the PS2.M−hemin complex reacts with H_2O_2 to yield a radical likely localized to the PS2.M oligonucleotide.[7] Although the precise mechanism for the peroxidase reaction leading to the generation of this radical was not fully elucidated, the PS2.M−hemin complex clearly reacted with H_2O_2 to produce an oxidant capable of oxidizing substrates (such as ABTS) in a catalytic reaction.[2,3] As discussed in the Introduction, the use of EPR to study organic hydroperoxide degradation mediated by heme-containing systems is reported to successfully yield mechanistic data for this peroxidase process. Thus, we have used *t*-Bu-OOH to determine the precise mechanism for the reaction of the PS2.M−hemin complex and organic hydroperoxides.

Heterolytic Cleavage of *t*-Bu-OOH by the PS2.M−Hemin Complex. The mechanism of hydroperoxide degradation by both hemin alone and heme proteins is an area of considerable debate in the literature. Despite the large number of studies, the precise mechanism(s) of alkyl peroxide decomposition and the identity of radical product(s) produced from this reaction are not clear. The classical "peroxidase" mechanism suggests that peroxides can be reduced in a two-electron reduction process to give the corresponding alcohol [reaction 1] and a compound I intermediate. This intermediate may then react further with the peroxide to yield a variety of secondary radical products including peroxyl, alkoxyl, and carbon-centered radicals [reactions 2 and 3]. Thus, with the exception of the nitroxide radical, a heterolytic mechanism appears to account for the distribution of radicals and the concomitant changes in the electronic spectra detected in the reaction of PS2.M−hemin and *t*-Bu-OOH. These data, together with the report[7] that reaction of PS2.M−hemin complex and H_2O_2 also showed a DNA oligonucleotide-derived radical and loss of the Soret intensity analogous to that for the corresponding reaction of HRP and H_2O_2,[24−26] are also supportive of the idea that *t*-Bu-OOH degradation in the presence of the PS2.M−hemin complex may occur by a heterolytic mechanism yielding a porphyrin π-radical cation.

However, the "classical" peroxidase mechanism cannot entirely account for the selective trapping of alkoxyl radicals from the reaction of PS2.M−hemin complex and *t*-Bu-OOH in the presence of increasing concentrations of DMPO. The preferential trapping of species assigned as *tert*-butyloxyl over those assigned as peroxyl radicals is the opposite of that anticipated by the product distribution predicted from the "classical" peroxidase mechanism. Extrapolating the yield of *tert*-butyloxyl and methyl peroxyl radicals (Figure 6) to concentrations of DMPO greater than 250 mM would yield mole fractions of *tert*-butyloxyl adducts approaching 100%, while that for the peroxyl radical (and also the nitroxide radical) would approach 0%. Overall, this preferential trapping of *tert*-butyloxyl radicals indicates that the alkoxyl radical is the primary species produced from the PS2.M−hemin complex-mediated scission of the organic peroxide. Only when sufficiently high concentrations of DMPO are employed can the spin trap compete with the kinetics of reactions leading to secondary radical products such as methyl, methyl peroxyl, and nitroxide radicals.

In addition, the definitive assignment of a putative porphyrin radical cation (i.e., a compound I) in the reactions of PS2.M−hemin and *t*-Bu-OOH cannot be made on the basis of the evidence obtained from the light absorption studies. For example, similar to the case for the corresponding reaction with hydrogen peroxide,[7] the time-dependent loss of the Soret in the reaction of PS2.M−hemin complex and *t*-Bu-OOH may also be interpreted as evidence for significant heme degradation. Such degradation of the heme group also leads to the time-dependent changes in the optical spectra noted here in the reaction of PS2.M−hemin and *t*-Bu-OOH and previously with H_2O_2,[7] thereby introducing ambiguity in the interpretation of these data. Overall, on the basis of the combined EPR and optical spectroscopic data, we conclude that *t*-Bu-OOH degradation by the PS2.M−hemin does not occur by a heterolytic mechanism. Therefore, in agreement with our recent study,[7] we conclude that the reaction of PS2.M−hemin and peroxide proceeds without formation of a compound I-like species.

***t*-Bu-OOH Degradation by the PS2.M−Hemin Complex through Metal-Mediated Hydrogen Abstraction**. By way of a similar argument to that presented above, the DMPO-dose-dependent results obtained here with the reaction of *t*-Bu-OOH and the PS2.M−hemin complex also conflict with the idea that peroxide degradation occurs by a hydrogen abstraction mechanism [reactions 5 and 6]. That is, the observation that only the relative mole fraction of the *tert*-butyloxyl−DMPO adduct continued to increase with increasing dose of spin trap, as opposed to the predicted increase in both *tert*-butyloxyl and peroxyl radical adducts of DMPO, supports the argument that *t*-Bu-OOH degradation does not occur by processes shown in reactions 5 and 6.

Homolytic Cleavage of *t*-Bu-OOH by the PS2.M−Hemin Complex. Consistent with data previously reported for cytochrome P450 and cytochrome *c*,[15,28] the data shown here on the degradation of an organic peroxide by the PS2.M−hemin complex largely support the idea that *t*-Bu-OOH degradation is mediated by the PS2.M−hemin complex through a homolytic cleavage of the O−O peroxy bond. That *t*-butyoxyl radicals are the primary radical trapped by DMPO at the highest ratio of DMPO/PS2.M−hemin complex tested and methyl peroxyl radicals are derived from the β-scission of these primary radicals supports this conclusion.

Despite the conclusion that PS2.M−hemin reacts with organic peroxides by the homolytic mechanism of peroxide degradation, there is increasing evidence indicating that other hemoproteins

that show peroxidase activity (e.g., both wild-type and mutant sperm whale myoglobins)[34] may react with peroxides by both homolytic and heterolytic mechanisms. Indeed, it is becoming increasingly evident that a variety of factors can influence the mechanism of peroxide degradation by heme-containing systems. For example, the extent of heterolysis reportedly depends on the pK_a[35] of the alcohol produced from the degradation reaction, while the extent of homolysis is apparently dependent on the stability of the radical produced from the β-scission reaction of the corresponding alkoxyl radical.[15] Also, the presence or absence of suitable reducing agents on the matrix adjacent to the heme prosthetic group either nearby or within the active site is also a key determinant of whether the second oxidation equivalent of compound I is found as a relatively unstable porphyrin π-radical cation or as a secondary radical species derived from the oxidation of the matrix.[34,36] Thus, the heme environment may also strongly influence which (if any) is the preferred mechanism of peroxide degradation.[37]

Interestingly, a recent report has strongly questioned the assignment of DMPO spin-trapped peroxyl radicals, suggesting that in many cases these dioxygen radicals cannot be trapped by DMPO at room temperature.[38] Indeed, Dikalov and Mason used oxygen-17 isotopic labeling to show that the DMPO adduct of the methyl alkoxyl radical was derived from the corresponding methyl peroxyl radical.[38] Whether this reassignment of organic peroxyl radical adducts holds true for peroxyl species derived from either secondary or tertiary carbon centers is not yet known. However if this were to be true, then the data presented in this study, and elsewhere in the literature,[14−19,28,39−42] would require significant reinterpretation. That is, if the radical assigned here as *tert*-butyloxyl were derived from the corresponding (and presumably unstable) peroxyl species, the data presented are consistent with the idea that peroxyl radicals are generated from the reactions of organic peroxides and the PS2.M−hemin complex consistent with heterolytic cleavage of the peroxide.

Another result from this study that warrants further discussion is the observation of triplet species obtained from the reaction of PS2.M−hemin and *t*-Bu-OOH in the presence of the spin trap. Because a DMPO adduct displaying coupling to only a single nitrogen atom has not been previously reported and the general structure of DMPO adducts by definition shows coupling to a β-hydrogen, it is unlikely that the triplet detected here is in fact an adduct of DMPO. It is more likely however that the radical is a free nitroxide species derived from PS2.M−hemin for two reasons. First, no radicals were detected in the absence of the PS2.M−hemin complex (Figure 2), and second, DMPOX and DMPO−OH were the only radicals detected from the reaction of DMPO and hemin alone. Site-specific oxidation of the nucleic acid guanine (G) at GG and GGG base sequences and subsequent cleavage of DNA are known to occur in the presence of hydroperoxides.[43−45] Our recent investigation of DNA strand damage on PS2.M in the presence of H_2O_2 supports the argument that PS2.M oligonucleotide undergoes site-specific guanine base oxidation in the presence of peroxide.[7] Therefore, it is conceivable that the oxidative damage to guanine may lead to the formation of a putative nitrogen-centered radical that in the presence of oxygen reacts to yield a free nitroxide radical. The marginal increase in the triplet signal observed in the absence of dioxygen (Figure 4), however, does not support this conclusion. Therefore, the precise identity of the nitroxide detected in this study remains to be determined.

Conclusion. On the basis of the majority of previous literature (however, for a conflicting view, see ref 36), the evidence provided in this study supports the conclusion that the PS2.M−hemin complex degrades *t*-Bu-OOH by scission of the O−O bond by a homolytic mechanism to yield *tert*-butyloxyl radicals as the primary radical species. The *tert*-butyloxyl radical appears to be the major radical adduct detected under conditions of high trapping efficiency that overcome rapid kinetic processes that give rise to secondary radicals. After the formation of this primary alkoxyl radical, β-scission yields methyl radicals that also react readily with oxygen to further yield methyl peroxyl radicals. In addition to the formation of *tert*-butyloxyl, methyl, and methyl peroxyl radical adducts, an as yet unidentified nitroxide radical is also detected in the reaction mixture.

Acknowledgment. This work was supported by Grant O 98S 0008 from the National Heart Foundation of Australia (to P.K.W.), CIHR Grant MT-7182 (to A.G.M.), and a Canada Research Chair (to A.G.M.).

IC010025E

(34) Allentoff, A. J.; Bolton, J. L.; Wilks, A.; Thompson, J. A.; Ortiz de Montellano, P. R. *J. Am. Chem. Soc*. **1992**, *114*, 9744−9749.
(35) Lee, W. A.; Bruice, T. C. *J. Am. Chem. Soc*. **1985**, *107*, 513−514.
(36) Miller, V. P.; Goodin, D. B.; Friedman, A. E.; Hartman, C.; Ortiz de Montellano, P. R. *J. Biol. Chem.* **1995**, *270*, 18413−18419.
(37) Shimizu, T.; Murakami, Y. Hatano, M. *J. Biol. Chem*. **1994**, *269*, 13296−13304.
(38) Dikalov, S. I.; Mason, R. P. *Free Radical Biol. Med*. **1999**, *27*, 864−872.
(39) Chamulitrat, W.; Takahashi, N.; Mason, R. P. *J. Biol. Chem*. **1994**, *264*, 7889−7899.
(40) Davies, M. J.; Slater, T. F. *Biochem. J*. **1987**, *245*, 167−173.
(41) Rosen, G. M.; Rauckman, E. J. *Mol. Pharmacol*. **1983**, *17*, 233−238.
(42) Kalyanaraman, B.; Mottley, C.; Mason, R. P. *J Biol. Chem*. **1983**, *258*, 3855−3858.
(43) Kawanishi, S.; Oikawa, S.; Murata, M.; Tsukitome, H.; Saito, I. *Biochemistry* **1999**, *38*, 16733−16739.
(44) Hazlewood, C.; Davies, M. J. *Arch. Biochem. Biophys*. **1996**, *332*, 79−91.
(45) Hazlewood, C.; Davies, M. J. *Biochem. Soc. Trans*. **1995**, *23*, 259S.